HTGAA 2026 · Individual Final Project · MIT · May 2026

AURA

KARINA FRANCES

LIFEFABS

Electromagnetic Sensing Textile Interface through Living Design

A biosynthetically grown second skin, reading the electromagnetic field energy of living environments

AURA wearable garments at three magnetic field frequencies: HZ 7.1, HZ 8, HZ 9, render.

SECTION 1: ABSTRACT

Every living system generates a bioelectrical signature. Plants propagate long-distance ionic calcium waves as structured electrical signals through tissue networks[1]; mycorrhizal fungal networks have demonstrated directional electrical signalling between organisms under field conditions[2]; and the Earth itself produces low-frequency geomagnetic resonances, specifically the Schumann resonance at approximately 7.83 Hz, overlapping with the human theta brainwave range[3]. Together, these ionic, geomagnetic, and electromagnetic phenomena constitute ancient environmental signals that shaped the sensory conditions within which vertebrate biology evolved.

In migratory species, magnetic field detection remains an active sensory mechanism, mediated by cryptochrome proteins via the radical-pair mechanism.[4] Human CRY2 belongs to the same protein family but was repurposed in vertebrates as a circadian clock regulator, leaving its magnetosensory architecture structurally intact but functionally silent.[4] In urban environments, anthropogenic electromagnetic noise has been shown to disrupt this cryptochrome-mediated compass in migratory birds.[5] Modern humans have no means of perceiving this electromagnetic difference at all.

AURA investigates this ecological and sensory disconnection through synthetic biology and wearable design. The project proposes a biosynthetic textile composed of a novel fusion protein, CsgA-CRY2-DrBphP, expressed in *E. coli* BL21(DE3) and self-assembled into a curli fibre matrix,[6] computationally designed to translate variations in ambient electromagnetic field conditions into dynamic chromatic outputs across the textile surface. The garment functions as a speculative interface: making otherwise imperceptible differences between living ecosystems, urban infrastructures, and industrial environments materially legible through the body.

Broad Objective: To computationally design, validate, and propose experimental testing for a biosynthetic wearable textile composed of a self-assembling CsgA-CRY2-DrBphP fusion protein matrix, hypothesised to detect variation in ambient geomagnetic and electromagnetic field characteristics and translate those variations into dynamic colour modulation mediated through bodily wear.

Hypothesis: Human CRY2 has been confirmed to form radical pairs in vitro when FAD is provided.[4] AURA hypothesises that this photochemistry survives assembly into an extracellular CsgA curli fibre, provided FAD is retained without cellular replenishment machinery. If cofactor occupancy is sufficient, variations in ambient magnetic field strength will alter the singlet-triplet interconversion rate of the FADH•/Trp• radical pair, triggering

conformational changes that propagate via the EAAAK×3 rigid linker to modulate DrBphP photoswitching between Pr (660 nm) and Pfr (740 nm), producing chromatic outputs across the textile surface proportional to the surrounding electromagnetic environment.

Specific Aims: Aim 1 (this project) designs and computationally validates the CsgA-CRY2-DrBphP fusion protein construct. Aim 2 expresses the construct in *E. coli* BL21(DE3) and validates CRY2 magnetosensory function through a four-stage spectroscopic protocol. Aim 3 scales the validated biomaterial into a complete wearable garment custom-fit to body geometry.

Methods: Benchling (construct design, restriction site analysis); UniProt/NCBI (sequence sourcing); IDT Codon Optimisation (CAI >0.80); AlphaFold 3 and ColabFold (structural prediction); Twist Biosciences (gene synthesis); pET-28a/BL21(DE3) (expression); UV-Vis spectrophotometry and Helmholtz coil (functional validation).

SECTION 2: PROJECT AIMS

Aim 1: Experimental Aim (this project)

The first aim computationally designs and digitally validates the CsgA-CRY2-DrBphP triple fusion protein. Benchling was used for construct assembly, reading frame verification, and restriction site analysis; UniProt/NCBI GenBank for sequence sourcing (CsgA P28307, CRY2 Q49AN0, DrBphP Q9RZA4); IDT Codon Optimisation for per-domain *E. coli* K12 optimisation (CAI >0.80); AlphaFold 3 and ColabFold for 3D structural prediction; and Twist Biosciences for gene synthesis via four-fragment Gibson Assembly into pET-28a (Addgene #69864-3).

Aim 2: Development Aim

Express CsgA-CRY2-DrBphP in *E. coli* BL21(DE3) and validate CRY2 quantum radical pair magnetosensory function through a four-stage spectroscopic protocol: (1) FAD fluorescence confirmation at ~520 nm; (2) $FADH^{\bullet}$ radical appearance at ~580 nm; (3) Helmholtz coil 0–500 μT magnetic field sensitivity assay; (4) DrBphP photoswitching rate comparison between the two-domain control and the full construct. A successful outcome would constitute the first experimental demonstration of cryptochrome quantum sensing within an extracellular self-assembled amyloid fibre, a result without precedent in the current literature.

Aim 3: Visionary Aim

From the validated textile, the visionary aim is to produce a complete wearable garment custom-fit to body geometry using 3D bioprinting of CsgA curli nanofibers as UV-free shear-thinning bioink.[7] The garment would incorporate a graduated pili array (3–17 mm),

designed from cantilever beam mechanics, to sense across the full target electromagnetic frequency range: from geomagnetic micropulsations in intact ecosystems to anthropogenic electromagnetic noise in urban landscapes. The array would be calibrated to the 7.83 Hz Schumann resonance and its harmonics.[3] This architecture draws conceptual inspiration from Clarke et al.'s discovery that bumblebees detect electric fields through mechanosensory hair deflection,[8] reconstructing an analogous sensing architecture biosynthetically in a wearable material.

Beyond passive detection, the curli amyloid scaffold's intrinsic electromagnetic shielding properties[6] would be tuned to selectively attenuate the anthropogenic radiofrequency noise that Engels et al. showed is sufficient to disrupt cryptochrome-mediated compass orientation in migratory birds.[5] The same field-dependent conformational changes in the pili array would simultaneously drive low-level electrodermal stimulation at skin contact points, translating detected Schumann-range frequencies into a direct haptic signal, with no neural modification required. Both applications are contingent on ISO 10993 biocompatibility clearance before any skin contact.

In its most developed form, a multiplexed array of spectrally distinct chromoproteins across differentiated pili zones would replace the current binary Pr/Pfr output with a continuous, body-mapped electromagnetic portrait of the wearer's environment. Further ahead, a redesigned fusion protein incorporating bioelectricity-sensitive domains, separate from the CRY2 magnetic sensing mechanism, could extend AURA's range to the ionic field signatures of living systems: the electrical flows of mycorrhizal networks[2] and the calcium wave propagation of plant stress responses,[1] making the body itself an instrument through which the electromagnetic language of living environments is, for the first time, materially perceptible.

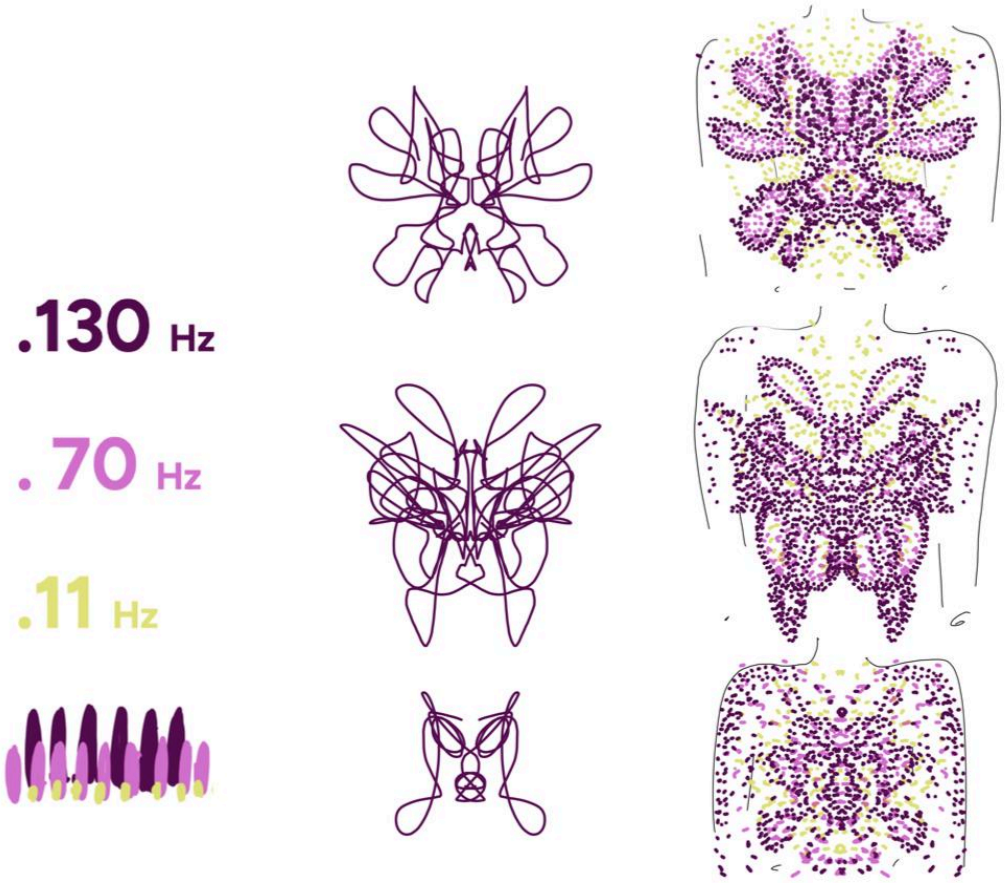

Visionary Aim Sketch

SECTION 3: BACKGROUND

Literature Context

Primary Citation 1: Foley et al. (2011)[9]

Foley, Gegear, and Reppert created transgenic *Drosophila* in which native cryptochrome was replaced by human CRY2. The flies sensed and responded to a coil-generated static magnetic field in a light-dependent manner consistent with the radical pair mechanism,[9] establishing that magnetosensory capacity is a property of the CRY2 protein domain itself, independent of its host cell or species. Whether humans possess the neuronal pathways to exploit this capability was left open;[9] AURA circumvents the question entirely by translating the sensing signal into colour output via DrBphP, bypassing neural processing altogether. Critically, Foley et

al. expressed CRY2 inside living neurons with full cellular support. AURA proposes to test whether the same function survives in an extracellular fibre, a context those authors did not address.

Primary Citation 2: Xu et al. (2021)[10]

Xu et al. provided the first direct experimental confirmation of cryptochrome radical pair magnetosensitivity outside a living organism, measuring the magnetic field sensitivity of robin CRY4 expressed and purified in solution.[10] Robin CRY4 proved quantitatively more magnetically sensitive than CRY4 from non-migratory species, providing evolutionary evidence that the radical pair mechanism is the genuine magnetic compass. This is the closest published precedent for AURA: if CRY4 radical pair chemistry functions in purified solution, CRY2 may function in an extracellular curli fibre, though that assembled fibre context remains entirely untested. The entire Aim 2 four-stage spectroscopic protocol is modelled on Xu et al.'s methodology.[10]

Novelty

The CsgA-CRY2-DrBphP fusion protein has no precedent in the literature. No prior work has placed human CRY2 in an extracellular self-assembling fibre context or proposed it as a user-worn environmental biosensor. The biliverdin-from-sweat hypothesis, in which the garment's chromophore is continuously resupplied by the wearer's own sweat as a haem catabolism product, has never been proposed for any living material. AURA introduces a new application category for synthetic biology: perceptual restoration, recovering a vestigialised molecular sensing capacity[4] through external material architecture rather than genetic modification. This is architecturally inspired by Clarke et al.'s identification of electric field detection via mechanosensory hairs in bees[8] and Sutton et al.'s characterisation of their weak electric field sensitivity,[11] reconstructing an analogous sensing architecture biosynthetically in a wearable material.

Why This Project Matters

Problem addressed: Modern humans inhabit electromagnetic environments fundamentally different from the living ecosystems in which vertebrate sensory biology evolved, yet have no sensory access to that difference. AURA proposes to close that gap through a biosynthetic material interface rather than genetic modification.

Advancement of knowledge: Aim 2 would constitute the first experimental test of whether cryptochrome radical pair quantum chemistry, demonstrated in living neurons[9] and in purified solution,[10] survives assembly into an extracellular self-assembling amyloid fibre matrix. A positive result would expand the known material contexts in which quantum biology can operate.

Field-level change: This project establishes engineered living materials as a viable platform for human sensory interface design: not merely structural fabrics, but active, adaptive perceptual interfaces that extend the human sensory vocabulary.

Ethical Implications

1. Material Safety (Non-Maleficence)

The CsgA curli fibre mat is a novel biomaterial with no published skin contact safety profile. No epidermal contact will occur until full ISO 10993 biocompatibility, toxicity, and allergen testing are complete.

2. Environmental Containment (Biosafety)

All phases use disabled BSL-1 *E. coli* strains incapable of survival outside a controlled laboratory environment.

3. Scientific Honesty (Pseudoscience Risk)

The electromagnetic sensing narrative could be misappropriated by the wellness market. The project maintains a strict published distinction between what Foley et al.[9] and Xu et al.[10] demonstrated and what AURA hypothesises. These are distinct claims and must never be presented as equivalent.

4. Biometric Data Sovereignty

Because the garment consumes endogenous biliverdin from the wearer's sweat, it unintentionally interfaces with private metabolic outputs. Strict privacy frameworks are required to prevent personal metabolic data from being tracked or exploited.

5. Eco-Somatic Alienation

Continuous haptic feedback of urban electromagnetic noise could cause psychological distress rather than reconnection. This risk must be addressed in the interaction design before public deployment.

6. Distributive Justice

Early iterations will be expensive. If sensory restoration and protection from harmful electromagnetic environments become exclusive to the wealthy, the project's core purpose is undermined. Equitable access must be designed in from the outset.

SECTION 4: EXPERIMENTAL DESIGN, TECHNIQUES, TOOLS, AND TECHNOLOGY

Techniques Checklist

- ☑ DNA Construct Design
- ☑ Restriction Enzyme Digestion
- ☑ Databases (GenBank, NCBI, UniProt)
- ☑ Designing a Twist Order
- ☑ Protein Design
- ☑ Use of Benchling (Gibson's Assembly)
- ☑ Models and Notebooks (AlphaFold 3, ColabFold)
- ☑ Chassis Selection (BL21(DE3), DH5alpha)
- ☑ Plasmid Preparation (pET-28a)
- ☑ Bacterial Culturing
- ☑ Cell Free Reactions (PURExpress, Aim 2 Stage 2)
- ☑ Gibson Assembly (Aim 2)
- ☑ Primer Design or Selection
- ☑ Protein Purification (Ni-NTA His-tag)

HTGAA Industry Council companies: Addgene (expression vector); Twist Biosciences (gene synthesis); New England Biolabs (cloning enzymes and competent cells); MilliporeSigma (bacterial media and reagents).

Fusion Protein Architecture

CsgA-CRY2-DrBphP is a single novel fusion protein expressed in *E. coli* BL21(DE3) and cloned into pET-28a (Addgene #69864-3): 4,336 bp, 1,446 amino acids, 156,669.69 Da.

Domain	Source	Function	Linker to Next
His6-tag	Synthetic	Ni-NTA affinity purification	—
CsgA	*E. coli* (P28307)	Curli scaffold: secreted via Type VIII machinery, self-assembles extracellularly into a stable beta-helix amyloid fibre mat[6]	GGGGS×3 flexible

CRY2 (res. 1–491)	Human (Q49AN0)	FAD-binding photolyase homology domain; proposed radical pair magnetosensor[9,10]	EAAAK×3 rigid[12]
DrBphP	*D. radiodurans* (Q9RZA4)	Biliverdin-bound bacteriophytochrome colour reporter; photoswitches between Pr (660 nm) and Pfr (740 nm)[13]	—
FLAG-tag	Synthetic	C-terminal orientation confirmation via anti-FLAG western blot	TAA stop codon

Table 1: Domain architecture of the CsgA-CRY2-DrBphP fusion protein. GGGGS×3 provides assembly freedom; EAAAK×3 provides rigid conformational transmission per Chen et al.[12]

Table 1: Domain architecture of the CsgA-CRY2-DrBphP fusion protein. GGGGS×3 provides assembly freedom; EAAAK×3 provides rigid conformational transmission per Chen et al.[11]

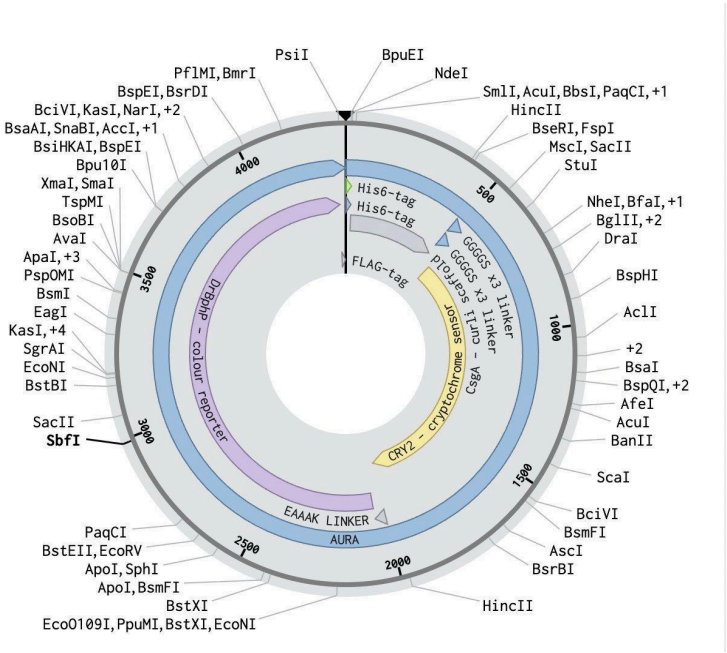

Transfer Plasmid (CsgA-CRY2-DrBphP)

Figure 1: Benchling annotated triple fusion plasmid map of AURA construct (CsgA-CRY2-DrBphP) (4,336 bp). His6-tag (green), CsgA (blue), GGGGS×3 linker (grey), CRY2 (yellow), EAAAK×3 linker, DrBphP (purple), FLAG-tag. ***https://benchling.com/s/seq-w7X4eQm6ddvncFWLqzwZ?m=slm-QMgJaJiFtloeHvfyYMaW***

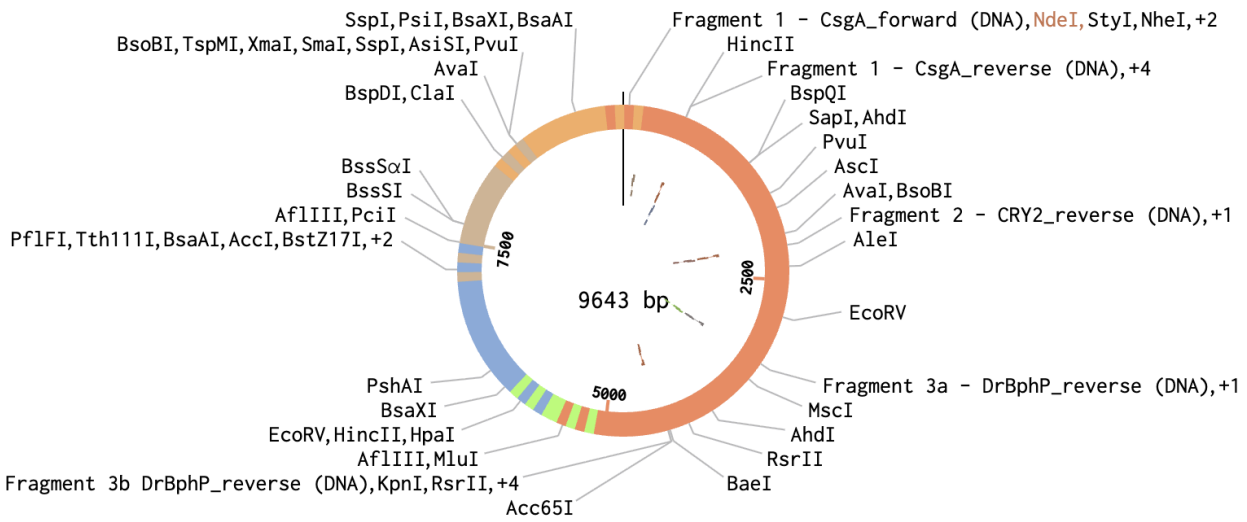

AURA Complete Expression Plasmid (CsgA-CRY2-DrBphP)/ pET-28a

Figure 2: Complete AURA expression plasmid (9,643 bp). pET-28a(+) backbone (Novagen, Cat. #69864-3; 5,369 bp) carrying the CsgA-CRY2-DrBphP triple fusion insert (4,336 bp) via four-fragment, cloned into NdeI/XhoI restriction sites via Gibson Assembly.

https://benchling.com/karinafrancesedmonds/f/lib_PgkHIFzcp0-quantderm/assem_lbRpCsLEWA-complete-aura-gibson-assembly/edit

Protein Fragment List (Viable for Twist)

Fragment	Primer	Sequence	Tm (°C)	Status
F1 CsgA forward	5'	AGTGGTGGTGGTGGTGGTGCCATATGGCTAGCATGACTGGT	72.43	✓
F1 CsgA reverse	3'	CCACCACCACTACCACCACCACCACCACCACTACCACCAC	72.98	✓
F2 CRY2 forward	5'	GTGGTGGTAGTGGTGGTGGTGGTGGTGGTAGTGGTGGTGG	72.98	✓
F2 CRY2 reverse	3'	GCTTCTTTTGCTGCAGCTTCCGCTTCTTTCGCCGCCGCTT	73.87	✓

F3a DrBphP forward	5'	AAGCGGCGGCGAAAGAAGCGGAAGCTGCAGCAAAAGAAGC	73.87	✓
F3a DrBphP reverse	3'	TGCCAACGTCCTTCAAAACGTAAGATCAGCCCTCCAGCAC	70.15	✓
F3b DrBphP forward	5'	GTGCTGGAGGGCTGATCTTACGTTTTGAAGGACGTTGGCA	70.15	✓
F3b DrBphP reverse	3'	CTGGTGCCGCGCGGCAGCCATTTATCATCGTCATCTTTATAGTCGG	72.15	✓

CsgA — Curli Fibre Scaffold

CsgA self-assembles extracellularly into a stable beta-helix amyloid fibre mat via the Type VIII secretion system.[6] In AURA it serves as the structural backbone of the textile, expressed N-terminally to preserve its secretion signal; without it, the entire material concept fails. CsgA fusions with functional cargo have been demonstrated at yields of 50–200 mg/L in *E. coli*,[6] though cargo of 1,274 amino acids exceeds published precedent and remains an open experimental question.

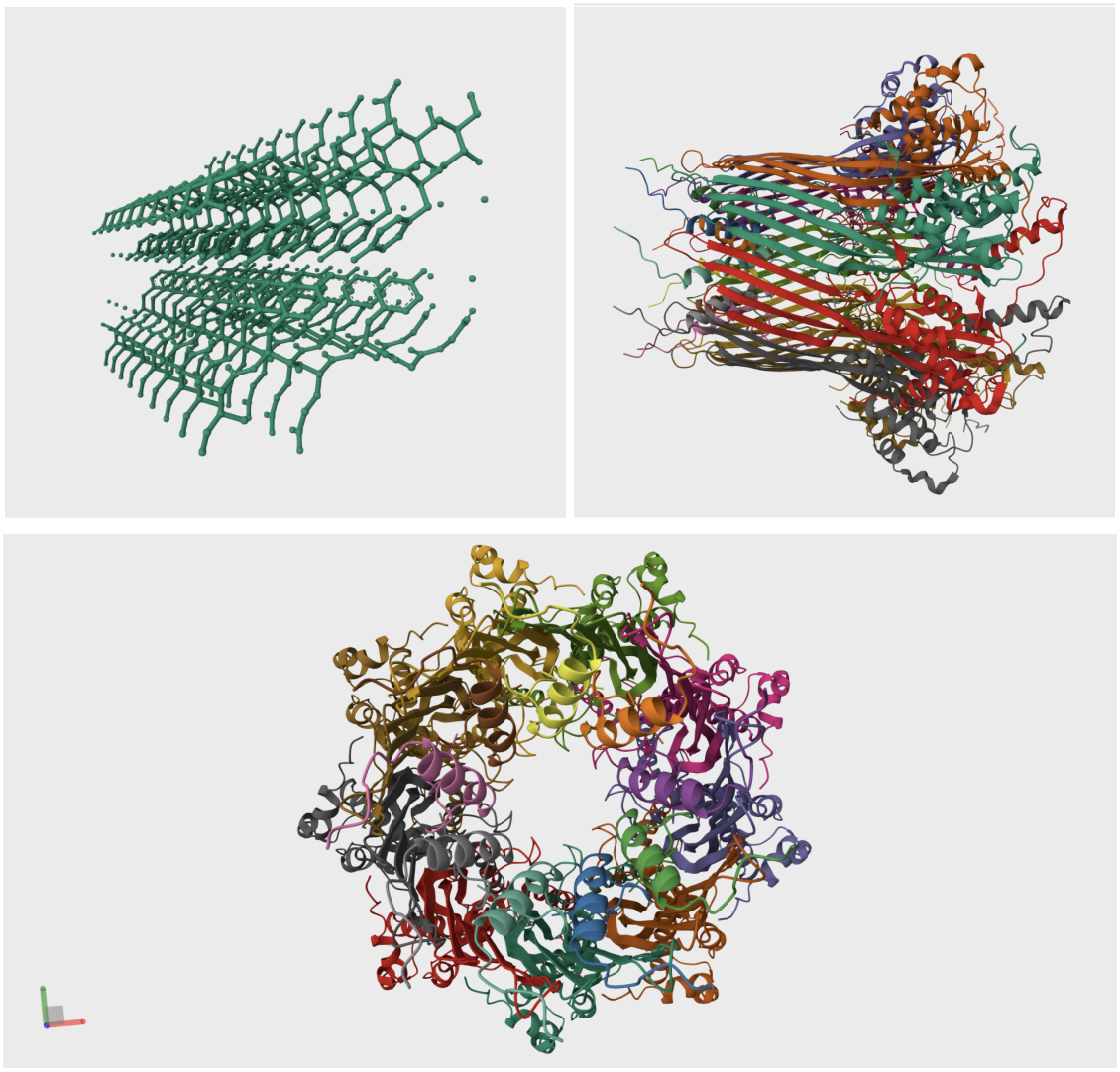

Figure: CsgA curlin major subunit (UniProt P28307). Crystal structure showing the characteristic beta-helix amyloid architecture. In AURA, CsgA serves as the structural scaffold: secreted via the Type VIII machinery and self-assembling extracellularly into the fibre mat.[6]

CRY2 — Cryptochrome Magnetosensor

Human CRY2 (UniProt Q49AN0, residues 1–491) is the FAD-binding photolyase homology domain proposed to function as the magnetic sensor in AURA. In magnetosensory cryptochromes, blue light absorbed by the FAD cofactor initiates electron transfer along a chain of four conserved tryptophans from the FAD outward to the protein surface, generating spin-correlated radical pairs whose singlet-triplet interconversion ratio is sensitive to applied

magnetic fields.[9,10] In vertebrates, CRY2 was repurposed as a circadian clock repressor,[4] leaving this electron transfer architecture present but inactive. Kutta et al.[4] demonstrated that FAD binding and radical pair photochemistry remain structurally possible in human CRY2 in vitro, which is the direct scientific basis for Aim 2. However, CRY2 binds FAD weakly (Kd 68 μM) and has no cellular machinery to replenish it once assembled into an extracellular fibre, making cofactor retention the primary biochemical risk of the project. Foley et al.[9] showed that human CRY2 retains magnetosensory capability in an appropriate biological context; AURA tests whether that capability survives outside one.

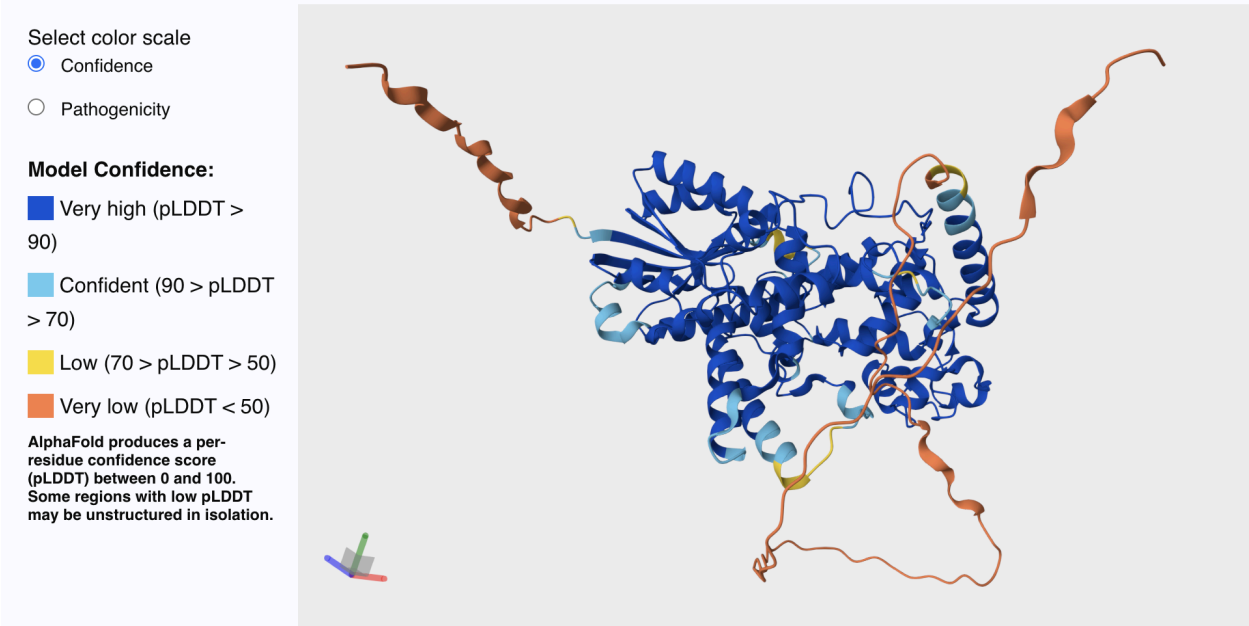

Figure: Human CRY2 (UniProt Q49AN0, residues 1–491). AlphaFold predicted structure (AF-Q49AN0-F1). Blue = high confidence; orange = low confidence. Proposed radical pair magnetosensor in AURA.

DrBphP — Colour Reporter

DrBphP was selected for four reasons: (1) high-resolution crystal structures available (PDB 4O0P, 4GW9); (2) clean Pr/Pfr switching with well-separated absorption maxima; (3) evolved in the most radiation-resistant organism known; (4) BphO, the heme oxygenase producing biliverdin, is co-encoded in the same *D. radiodurans* operon, enabling endogenous chromophore production during expression.[13]

Output limitation: Pr (660 nm) and Pfr (740 nm) are near-infrared; Version 1 requires NIR imaging. Future versions would substitute a visible-range phytochrome reporter.

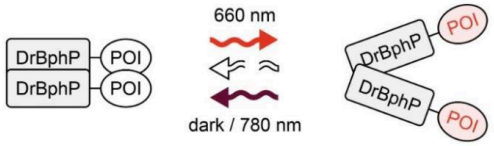

Photoreceptor	DrBphP
Binding partner	/
Cofactor	Biliverdin
Source organism	*Deinococcus radiodurans*
Mode of action	homodimerization, dissociation
Excitation wavelength	660 nm
Reversion wavelength	780 nm, dark

Crystal structure of DrBphP, Pr state. (PDB ID: 4O0P)

Figure: DrBphP photoreceptor schematic. Left: photoswitching: 660 nm drives Pr→Pfr; dark/780 nm reverts to Pr homodimer. Right: crystal structure, Pr state (PDB: 4O0P). Cofactor: biliverdin.[12]

Detailed Experimental Plan with Timeline

1. **Domain sequence sourcing (Day 1):** Download CsgA (P28307), CRY2 Q49AN0 residues 1–491, DrBphP Q9RZA4 from UniProt/NCBI GenBank. Verify against published literature.[4,6,12] Expected: sequences matching published functional residues.
2. **Codon optimisation (Day 1–2):** Submit each domain separately to IDT Codon Optimisation (*E. coli* K12). Expected: CAI >0.80 per domain.
3. **Linker design (Day 2):** Design GGGGS×3 at CsgA–CRY2 junction (flexible, assembly freedom) and EAAAK×3 at CRY2–DrBphP junction (rigid, conformational transmission per Chen et al.[12]). Expected: EAAAK×3 confirmed as stable alpha-helix by AlphaFold secondary structure prediction.[12]
4. **Construct assembly in Benchling (Day 2–3):** Assemble full 4,336 bp sequence in pET-28a backbone with NdeI/XhoI cloning sites. Verify reading frame, start/stop codons. Expected: single continuous reading frame, no frameshifts.
5. **Restriction site analysis (Day 3):** Run Benchling restriction site mapping. Identify and eliminate internal NdeI sites (CATATG). Two sites found at positions ~42 and ~825; eliminated by synonymous CAT→CAC substitution. Expected: no internal NdeI sites in final construct.
6. **AlphaFold 3 structural prediction (Day 3–4):** Submit full fusion as a five-chain multimer. Expected: EAAAK×3 as continuous alpha-helix per Chen et al.;[12] CRY2 mixed

alpha/beta photolyase fold per Kutta et al.;[4] C24 biliverdin attachment site confirmed in DrBphP domain per Bhoo et al.[13]

7. **Tryptophan tetrad mapping (Day 4):** Map all 17 tryptophans in CRY2 Q49AN0 residues 1–491. Identify tetrad candidates by positional homology with *Drosophila* CRY[9] and robin CRY4a.[10] Expected: 6 strongest candidates at W311, W358, W371, W390, W393, W416/W418.
8. **Protein properties calculation (Day 4):** Calculate MW, pI, net charge, instability index using Benchling ProtParam. Expected: MW 156,669.69 Da, pI 5.81, net charge −25.85 at pH 7.4, instability index 42.82. The net charge of −25.85 directly informs the Aim 2 biliverdin loading protocol: electrostatic repulsion between the negatively charged fibre surface and negatively charged biliverdin will require adjusted buffer ionic strength.
9. **Twist Biosciences submission (Day 5–7):** Three successive failures occurred before a viable strategy was achieved (see Section 5 Challenges). The long direct repeats intrinsic to CsgA amyloid domain architecture[6] drove the primary failure. Resolved by splitting into four fragments with synonymous codon diversification of the EAAAK repeats and CAT→CAC substitution at two internal NdeI sites.
10. **Gibson Assembly strategy (Day 7):** Four-fragment Gibson Assembly into NdeI/XhoI-linearised pET-28a: Fragment 1 CsgA (507 bp), Fragment 2 CRY2 (1,515 bp), Fragment 3a DrBphP first half (1,155 bp), Fragment 3b DrBphP second half (1,179 bp).
11. **[Aim 2] Expression (Week 2–3):** Transform pET-28a into BL21(DE3) by heat shock; plate on LB-agar + kanamycin 50 µg/mL overnight at 37°C. Expand to 1 L at 37°C, 200 rpm. At OD600 0.6, induce with IPTG 0.5 mM + biliverdin 25 µM + FAD 200 µM. FAD at 200 µM is ~3× the CRY2 Kd of 68 µM,[4] ensuring >50% cofactor occupancy, the minimum for detectable radical pair chemistry.[4,14] Reduce to 18°C; express 24 hours. Harvest at 5,000 × g, 10 min, 4°C. Expected: curli fibre mat visible at 48 hours; 20–80 mg/L after Ni-NTA purification,[6] confirmed by SDS-PAGE (~156 kDa) and anti-FLAG western blot.
12. **[Aim 2] Stage 1 — Colour-changing fibre checkpoint (Week 3):** Validate CsgA-DrBphP two-domain construct (no CRY2) as a pass/fail checkpoint before introducing quantum sensing complexity. Resuspend washed fibre mat to OD600 0.5 in PBS pH 7.4.[6] Record baseline absorbance 600–800 nm in darkness. DrBphP is canonical: Pr is the dark-adapted ground state, absorbing at 660–700 nm.[13] Illuminate with 660 nm LED (5 mW/cm², 120 s) off-axis to drive Pr→Pfr;[13] record absorbance immediately after. Monitor dark reversion every 5 minutes for 60 minutes minimum. DrBphP Pfr→Pr thermal reversion operates on a 45–90 minute timescale.[13] Pass criterion: unambiguous absorbance increase at 740 nm and decrease at 660–700 nm post-illumination, with progressive reversion over the 60-minute monitoring period. Control: CsgA-only construct. Do not proceed until passed.
13. **[Aim 2] Test 1 — FAD confirmation (Week 4):** Excite full CsgA-CRY2-DrBphP fibre mat at 450 nm; record emission 470–650 nm.[10] Wash three times in PBS pH 7.4 and repeat

to distinguish CRY2-bound from free FAD.[4] Pass criterion: fluorescence emission at 520 nm ± 5 nm, SNR ≥ 3:1, persisting after washing.[4,10] Control: CsgA-DrBphP without CRY2; any 520 nm signal here indicates contaminating free FAD. Failure response: increase FAD to 400 µM; if absent, proceed to FAD binding pocket mutagenesis before Test 2.[4]

14. **[Aim 2] Test 2 — Radical pair formation (Week 4):** Degas FAD-confirmed fibre mat by argon bubbling for 5 minutes to minimise oxygen-mediated radical quenching.[10] Use a pulsed 455 nm high-power LED (10–25 mW/cm²) positioned off-axis from the spectrophotometer beam. Deliver 1–10 second pulses and shutter between pulses to record spectra; simultaneous continuous illumination and absorbance measurement at 450 nm are not possible, as the LED source overlaps with the measurement wavelength and corrupts the signal. Monitor FAD bleaching at 450 nm and FADH• neutral semiquinone accumulation across 500–700 nm (~580 nm primary indicator) over 120 seconds total illumination.[10] Record 580 nm decay in darkness for 120 seconds to establish baseline k_0 for Test 3.[10] Pass criterion: measurable decrease at 450 nm and new increase at ~580 nm, both above instrument noise. Controls: CsgA-DrBphP without CRY2 (no 580 nm increase expected); boiled construct (both signals absent). Bleaching without 580 nm peak indicates disrupted tryptophan electron transfer: proceed to tetrad mutagenesis per Table 3.[9,10]
15. **[Aim 2] Test 3 — Magnetic field sensitivity (Week 5):** Apply static fields of 0, 50, 100, 200, 350, and 500 µT sequentially via Helmholtz coil, using Earth's ambient ~50 µT as a physiological reference point.[15] At each field strength, repeat the Test 2 pulsed illumination protocol and record FADH• decay kinetics at ~580 nm with the field held constant. Fit each decay curve to a single exponential to extract rate constant k. If CRY2 is magnetically sensitive in this fibre context, the applied field will alter the singlet-triplet interconversion rate of the radical pair, producing a field-dependent shift in k.[9,10,15] Pass criterion: monotonic relationship between field strength and k, $R^2 \geq 0.85$, $p < 0.05$ across six field strengths.[10] Control: full field series on CsgA-DrBphP without CRY2; no field-dependent change is expected.[9]
16. **[Aim 2] Test 4 — DrBphP modulation (Week 5):** Illuminate both CsgA-DrBphP control and full CsgA-CRY2-DrBphP construct with 660 nm LED (5 mW/cm², 120 s);[13] monitor 740 nm absorbance in real time to extract Pfr accumulation rate constant for each. Repeat under 200 µT applied field.[10] Pass criterion: measurable rate difference between control and full construct, amplified under field. Rate difference at zero field confirms EAAAK×3 linker transmission of CRY2 conformational state to DrBphP;[12] field-dependence confirms the complete radical pair → conformational change → colour switching transduction chain.[9,10,12]

Equipment and Supply List — Aim 2

Equipment

- Incubator shaker (37°C and 18°C, 200 rpm)
- Spectrophotometer (OD600 measurement)
- Centrifuge, 5,000 × g, 4°C cooling
- UV-Vis spectrophotometer (dual-wavelength kinetic mode, 350–800 nm)
- Fluorescence spectrophotometer (excitation 450 nm, emission 470–650 nm)
- Quartz cuvettes (1 cm path length)
- Pulsed 455 nm high-power LED (e.g. Thorlabs M455L3) with shutter, off-axis mount
- 660 nm LED (5 mW/cm²)
- Light power meter
- Helmholtz coil (0–500 μT) with DC power supply
- Gaussmeter (field verification)
- Argon gas supply and bubbling apparatus
- Ni-NTA affinity chromatography column (HisTrap HP, Cytiva)
- SDS-PAGE electrophoresis system and western blot apparatus
- 42°C water bath (heat shock transformation)
- Biosafety cabinet (BSL-1)

Biological Materials

- pET-28a carrying CsgA-CRY2-DrBphP (full construct)
- pET-28a carrying CsgA-DrBphP (two-domain control; Stage 1, Tests 2–4)
- pET-28a carrying CsgA-only (Stage 1 specificity control)
- E. coli BL21(DE3) competent cells (NEB)
- E. coli DH5α competent cells (plasmid propagation)

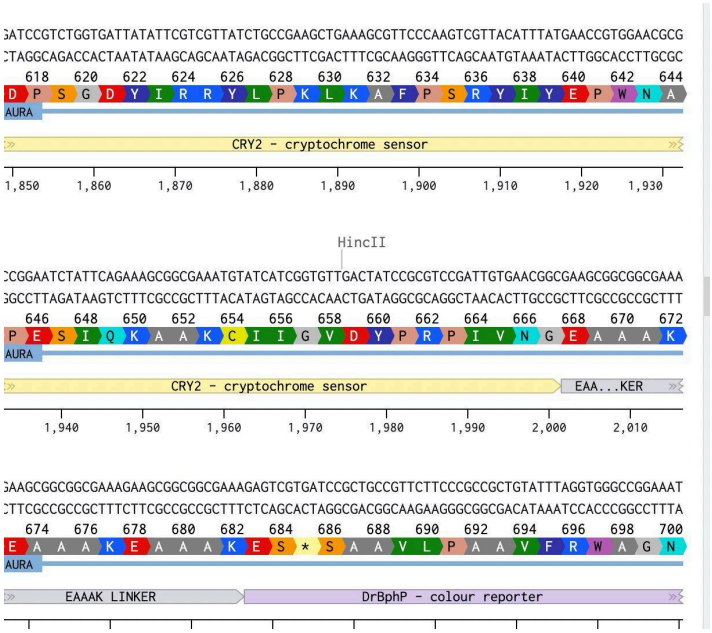

Figure 2: Benchling sequence view at the CRY2–EAAAK linker junction. EAAAKEAAAKEAAAK at the CRY2 C-terminus, transitioning into DrBphP.

Technique Expansion 1: DNA Construct Design

The construct required a 4,336 bp coding sequence with three functional domains in the correct order. CsgA must sit N-terminal to preserve its Type VIII secretion signal; without it, the material concept fails before any sensing question can be asked. The two linkers serve opposite mechanical roles: GGGGS×3 provides conformational freedom at the CsgA–CRY2 junction, while EAAAK×3 provides rigid conformational transmission at the CRY2–DrBphP junction, as established by Chen et al.[12] The construct was confirmed using Benchling reading frame analysis, per-domain codon optimisation (CAI >0.80), and restriction site mapping. Two unexpected internal NdeI sites were identified and removed by synonymous CAT→CAC substitution before gene synthesis.

Technique Expansion 2: Protein Design using AlphaFold 3

AlphaFold 3 was used to structurally validate the fusion construct before any wet lab work. Submitted as a five-chain multimer (ipTM 0.19, pTM 0.43), secondary structure analysis confirmed the EAAAK×3 linker as a single continuous alpha-helix, consistent with its designed role as a rigid transmission element per Chen et al.[12] Benchling ProtParam returned a net charge of −25.85 at pH 7.4. Since biliverdin is also negatively charged at physiological pH (both propionic acid side chains, pKa 3.9 and 5.3, are fully deprotonated), it will experience electrostatic repulsion from the fibre surface, directly informing the Aim 2 biliverdin loading protocol. Finally, a tryptophan map of all 17 residues in CRY2 Q49AN0 (residues 1–491) was generated, identifying the strongest radical-pair tetrad candidates as a baseline for directed evolution following the structural comparison approach of Xu et al.[10]

DNA construct design was the foundational technique of Aim 1, requiring a 4,336 bp coding sequence with three functional domains in the correct order. CsgA must sit N-terminal to preserve its Type VIII secretion signal required for extracellular fibre assembly; if this is disrupted, the entire concept fails before any sensing question can be asked. Two linkers were designed to serve mechanically opposite roles: GGGGS×3 at the CsgA–CRY2 junction for assembly freedom, and EAAAK×3 at the CRY2–DrBphP junction for rigid conformational transmission, based on systematic characterisation of linker mechanical properties by Chen et al.[11] The construct was verified using Benchling reading frame analysis, per-domain codon optimisation (IDT, CAI >0.80), and restriction site mapping, with two unexpected internal NdeI

SECTION 5: RESULTS & QUANTITATIVE EXPECTATIONS

What Aspect Was Validated?

Aim 1 validated the computational design and synthesis-readiness of the CsgA-CRY2-DrBphP fusion protein construct. Across fourteen design phases, the complete 4,336 bp coding sequence was digitally verified at both sequence level and structural level: four gene fragments were accepted by Twist Biosciences and confirmed ready for four-fragment Gibson Assembly; all key functional residues were confirmed including the DrBphP biliverdin attachment site (C24, fusion position 698) and a complete CRY2 tryptophan architecture map (17 residues); and AlphaFold 3 structural prediction confirmed the EAAAK×3 rigid linker as a single continuous alpha-helix and verified the biliverdin binding pocket geometry in the full fusion context.

AlphaFold 3 Structural Analysis

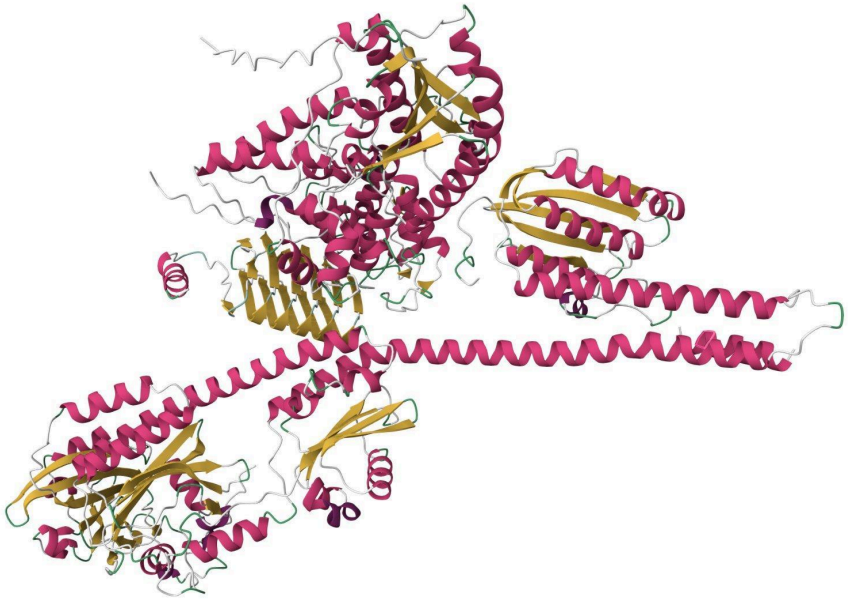

Figure 5a: Secondary structure of the full AlphaFold 3 multimer (ipTM 0.19). Pink = alpha helices; gold = beta sheets; grey = loops. The long continuous pink helix is the EAAAK×3 rigid linker, predicted as a single uninterrupted alpha helix.

Figure 5d: Full-protein hydrophobicity (AlphaFold 3, Mol viewer). Green = hydrophilic; red = hydrophobic. EAAAK helix shows amphipathic character. Floating DrBphP subdomain reflects AlphaFold uncertainty (ipTM 0.19), not a structural defect.*

Figure 5i: Chain D, EAAAK×3 rigid linker confirmed as alpha-helical (D | GLU 11). Spatial separation from the main protein body is an AlphaFold artefact (ipTM 0.19). Alphafold placement uncertainty.

Properties

Position	1-4338 (forward)
Summary	MHHH...DDDK* 1446 AAs
Molecular weight	156669.69 Da
Isoelectric point (pI)	5.81
Extinction coefficient	
Cys fully reduced	226660.00 $M^{-1}cm^{-1}$
Abs 0.1% (1 g/l)	1.447
Cys fully oxidized	227660.00 $M^{-1}cm^{-1}$
Abs 0.1% (1 g/l)	1.453
Instability index	42.82 (unstable)

Net Charge

pH	Charge
4	111.49
4.5	68.81
5	33.63
5.5	11.02
6	-6.01
6.5	-18.82
7	-25.85
7.5	-29.19
8	-31.70
8.5	-35.97
9	-44.54
9.5	-59.06
10	-79.39

Figure 3 (left): Protein properties: 1,446 aa, MW 156,669.69 Da, pI 5.81, instability index 42.82.

Figure 4 (right): Net charge at pH 4–10. Key value: −25.85 at pH 7.4, directly informing biliverdin loading protocol.

Biliverdin Binding Site Verification

Residue	DrBphP Position	Fusion Position	Context	Function
C24	24	698	TEN[C]ERE	Covalent biliverdin attachment; matches PDB 4GW9 exactly.
Y176	176	850	ML[Y]KF	Chromophore stacking: π–π interaction with biliverdin D-ring.
D207	207	881	AS[D]IP	Biliverdin D-ring propionate contact: hydrogen bond.
H260	260	934	PM[H]MQ	GAF domain histidine: coordinates biliverdin in Pr state.[13]
C289	289	963	LIA[C]HHQ	Secondary cysteine: structural role in GAF domain.

Table 2: DrBphP biliverdin-binding site verification. Fusion position = DrBphP residue + 674. Sequence presence confirmed; functional loading must be verified experimentally in Aim 2.

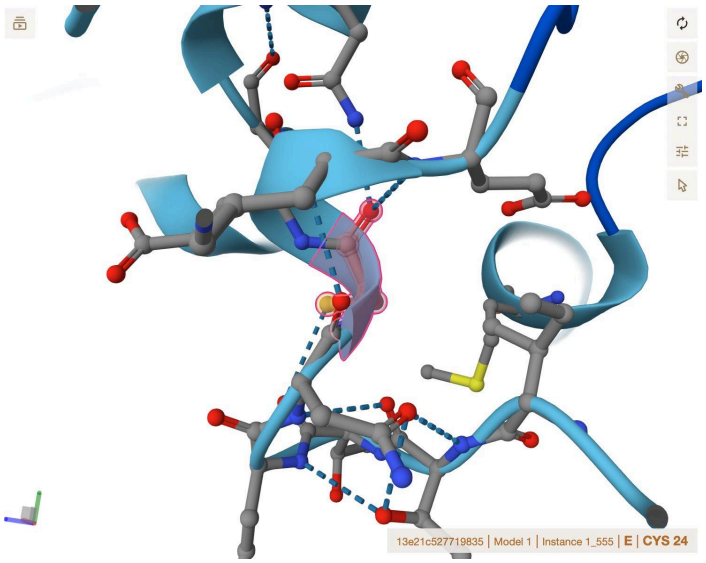

Figure 5h (top): DrBphP CYS 24 close-up showing sulfur atom (yellow) that forms thioether bond with biliverdin.[12]

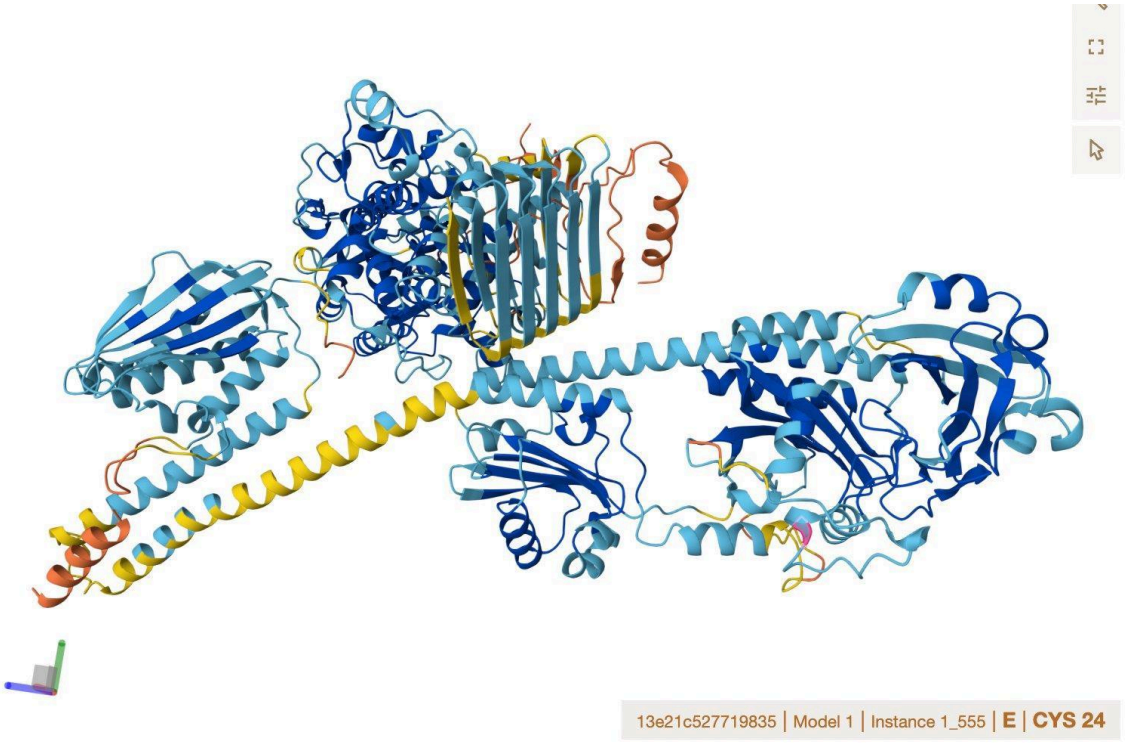

Figure 5h (bottom): Full protein with CYS 24 selected (pink marker, lower right of DrBphP domain).

AlphaFold Sequence Verification

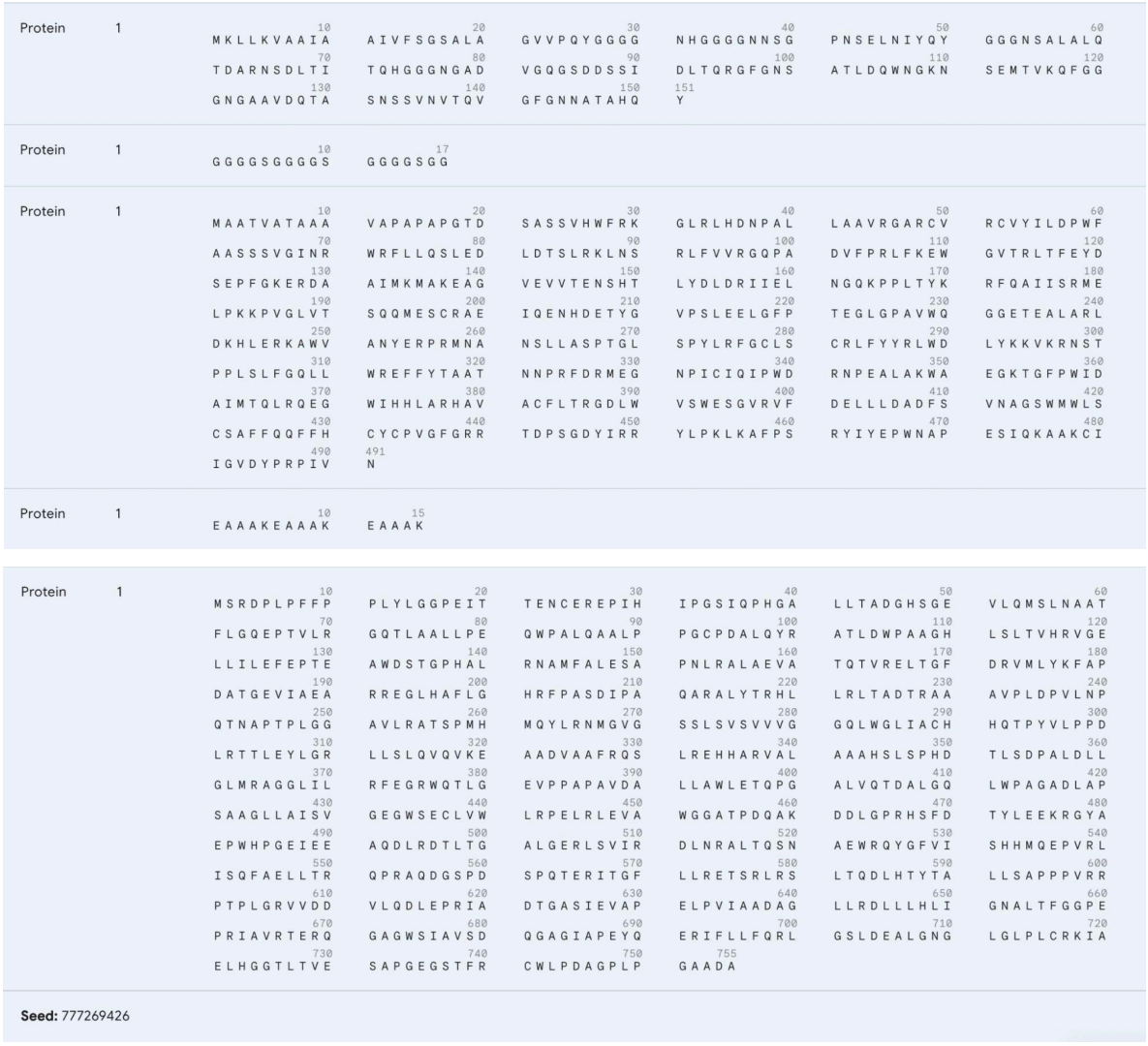

Figure 5g (top): All five chains submitted: CsgA (151 aa), GGGGS (17 aa), CRY2 (491 aa, Q49AN0), EAAAK (15 aa), and DrBphP chain (755 aa), confirming biliverdin attachment site at C24.

Tryptophan Architecture Map — CRY2

CRY2 Position	Chain C	Context	Region	Tetrad Candidate?
W27–W289	195–457	—	N-terminal / PHR core	No
W311	479	QLL[W]REF	FAD-proximal	Likely WA
W358	526	GFP[W]IDA	FAD-proximal	Likely WB
W371	539	QEG[W]IHH	FAD-proximal	Likely WB alt.
W390/W393	558/561	GDL[W]VSW / WVS[W]ESG	FAD-proximal	Likely WC, paired cluster
W416/W418	584/586	AGS[W]MWL / SWM[W]LSC	C-terminal surface	Likely WD, paired cluster
W467	635	YEP[W]NAP	C-terminal	No; directed evolution baseline

Table 3: Computational tryptophan architecture map of human CRY2 (UniProt Q49AN0, residues 1–491). The radical pair electron transfer chain runs sequentially WA→WB→WC→WD from FAD outward to the protein surface, generating the spin-correlated radical pair whose singlet-triplet interconversion ratio is sensitive to magnetic fields.[9,10,15] The exact tryptophan positions in human CRY2 have not been experimentally mapped; candidates here are identified by positional homology with the characterised chains of D. melanogaster CRY[9] and European robin CRY4a,[10] for which mutagenesis has confirmed the WA–WD positions. All assignments are computational predictions requiring site-directed mutagenesis for confirmation. If Tests 2 or 3 fail, this map provides the primary mutagenesis roadmap. Fusion position = CRY2 residue + 168.

Synthesis Results

FAIL 1: Full 4,336 bp sequence rejected. Four long direct repeats (≥13 bp) from CsgA amyloid domain architecture[6], intrinsic to curli structure and unmodifiable. Solution: split into three separate Gibson Assembly fragments.

FAIL 2: Fragment 3 rejected. The EAAAK×3 linker, consisting of three identical 15-amino-acid repeats, a 30 bp direct repeat in the coding sequence. Solution: synonymous codon diversification of each repeat (GAA/GAG/GAA for Glu; GCC/GCG/GCT for Ala; AAG/AAA/AAG for Lys), preserving the protein sequence while breaking up the repetitive DNA.

FAIL 3: Fragment 3 after EAAAK fix rejected. Natural repeats in DrBphP PAS-GAF-PHY domain at positions ~1,880–2,130. Solution: split into fragments 3a and 3b, making the final strategy a four-fragment Gibson Assembly.

FIXED: Two internal NdeI sites (CATATG) at positions ~42 and ~825, eliminated by synonymous CAT→CAC substitution. Reading frame and amino acid sequence unchanged.

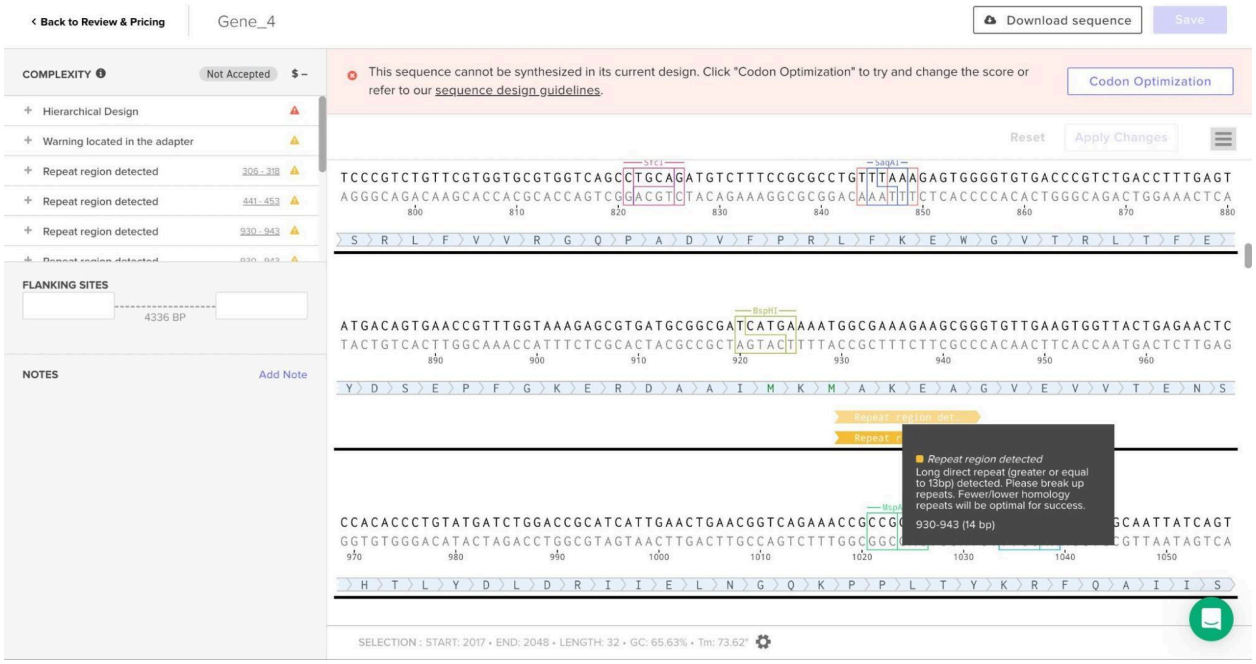

Figure 7: First Twist Biosciences submission, Not Accepted. Four direct repeat regions flagged (positions 306–318, 441–453, 930–943) from CsgA amyloid domain structure.[6]

Fragment	Length	Complexity	Price	Status
Fragment 1: CsgA	507 bp	Standard	$30.42	Accepted
Fragment 2: CRY2	1,515 bp	Complex	$90.90	Accepted
Fragment 3a: DrBphP first half	1,155 bp	Standard	$69.30	Accepted
Fragment 3b: DrBphP second half	1,179 bp	Complex	$70.74	Accepted
TOTAL	4,356 bp*	2× Standard, 2× Complex	**$261.36**	All accepted

*Table 4: Final Twist Biosciences synthesis order (Gene Draft 2). *4,356 bp includes Gibson Assembly overlap sequences; coding sequence is 4,336 bp.*

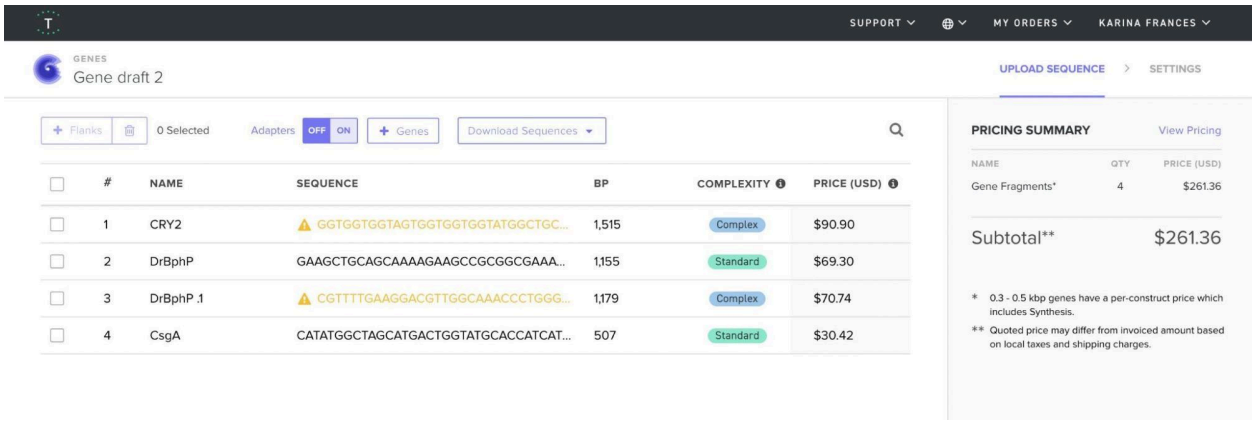

Figure 14: Twist Biosciences Gene Draft 2, all four fragments accepted, $261.36 total.

Synthetic Biology Techniques Utilised in Validation

The four primary techniques were DNA construct design, protein design, computational structural analysis, and gene synthesis. Benchling drove all fourteen design phases: reading frame verification, restriction site analysis, and codon optimisation (CAI >0.80 across all three domains). AlphaFold 3, submitted as a five-chain multimer, predicted the three-dimensional structure, confirmed secondary structure integrity, and verified the biliverdin binding site; Mol* viewer enabled systematic tryptophan mapping across the CRY2 domain. Acceptance of all four fragments by Twist Biosciences in Gene Draft 2 served as the practical validation

endpoint, confirming the sequence is free of long direct repeats, problematic GC content, and internal restriction sites that would block synthesis or cloning.

Aim 2: Proposed Quantum Sensing Protocol

What Is Being Measured

Spectroscopic readout (nm): A UV-Vis spectrophotometer measures absorbance or fluorescence emission of the fibre mat at specific wavelengths, revealing the redox chemistry inside the fibre at each stage.

Magnetic field stimulus (μT): Applied externally via Helmholtz coil. Not directly observable; it is detected by watching whether the FADH• decay rate at ~580 nm changes as field strength increases. The magnetic field alters the spin state of the FADH• radical pair, changing its decay rate. Whether that decay rate is field-dependent in this extracellular fibre context is the central question of Test 3.

- **450 nm:** FAD absorption peak. Bleaching here means FAD is being chemically reduced.
- **~520 nm:** FAD fluorescence emission (free FAD emits at ~525 nm in solution; binding within CRY2 shifts this slightly blue). A signal persisting after washing confirms FAD is retained within the fibre, not free in solution.
- **~580 nm:** FADH• neutral semiquinone radical absorption. A peak here confirms the flavin semiquinone has formed under blue-light illumination, consistent with radical-pair photochemistry. The exact position may shift depending on the CRY2 protein environment within the curli fibre and must be confirmed empirically in Stage 1.
- **660 nm / 740 nm:** DrBphP Pr and Pfr states. Switching between these confirms the colour reporter is responding.

Stage 1: Prove colour-changing fibre (no quantum complexity)

- Clone CsgA-DrBphP two-domain construct into pET-28a,[6] transform into BL21(DE3)
- Grow in LB + kanamycin 50 μg/mL at 37°C to OD600 0.6; add IPTG 0.5 mM + biliverdin 25 μM;[13] reduce to 18°C; express 24 hours
- Confirm DrBphP photoswitching at 660 nm (Pr) and 740 nm (Pfr) after 48-hour curli fibre mat assembly[6,12]
- Test biliverdin loading from simulated sweat at 10–100 nM, pH 7.4

Pass/fail checkpoint. If the fibre does not form or DrBphP does not photoswitch, the problem is expression or assembly, not sensing, and must be resolved before Stage 2.

Stage 2: Four-test quantum sensing protocol

Test	Applied	Measured	Pass Criterion
1. FAD confirmation	450 nm excitation	Fluorescence at ~520 nm	520 nm signal confirmed
2. Radical pair formation	Blue light 400–450 nm	Absorbance at 450 nm and ~580 nm over time	450 nm bleaches; 580 nm peak appears
3. Magnetic field sensitivity	0–500 μT (Helmholtz coil)	FADH• decay rate at ~580 nm per field strength	Decay rate changes with field strength
4. DrBphP modulation	660 nm illumination + field	Photoswitching rate vs CsgA-DrBphP control	Measurable rate difference

Table 5: Proposed Aim 2 four-stage quantum sensing protocol. Status: proposed, not yet executed.

Expected Outcomes

Measurement	Hypothesised Result	Significance if Observed
CsgA self-assembly	Fibre mat at 48 hours	Pass/fail checkpoint[6]
Expression yield	20–80 mg/L	Below 50–200 mg/L for single-domain CsgA;[6] large cargo may reduce efficiency
FAD at ~520 nm	Signal detected; may be weak	CRY2 retained FAD after extracellular fibre assembly.[9,10] Signal may be weak: human CRY2 binds FAD loosely (Kd 68 μM)[4] and lacks cellular replenishment in this context. A weak but persistent signal after washing is sufficient to proceed to Test 2; absence triggers the failure response protocol.

FADH• at ~580 nm	New peak under blue light	Radical pair photochemistry active in extracellular fibre[10]
Field-dependent decay	Decay rate varies with μT	CRY2 is magnetically sensitive in the fibre[9,15]
DrBphP modulation	Rate differs from control	EAAAK linker transmits CRY2 conformational events to DrBphP[12]

Table 6: Hypothesised Aim 2 outcomes. None have been experimentally verified.

Challenges Encountered and Potential Problems

The most significant challenge in Aim 1 was gene synthesis. Three successive Twist Biosciences submissions were rejected before a viable strategy emerged. Each failure required a different solution: fragment splitting, synonymous codon diversification, and internal restriction site removal, totalling fourteen design phases. This confirmed that biological constraints in curli and bacteriophytochrome sequences create synthesis problems that cannot be predicted from sequence alone.

Looking ahead to Aim 2, three primary risks remain: whether CsgA can drive extracellular self-assembly with 1,274 amino acids of cargo (significantly exceeding published precedent in Seker et al.[6]); electrostatic repulsion between the negatively charged fibre and biliverdin, which will require adjusted buffer ionic strength; and whether CRY2 radical pair function survives fibre assembly without cellular support, which is the central experimental risk of the project. If the fibre format fails, the scientifically consistent fallbacks are cell-surface display or a living-cell hydrogel scaffold.

Open Uncertainties

(1) CRY2 quantum coherence in an extracellular fibre

The central experimental risk is whether CRY2 radical pair function[9,10] survives assembly into a curli fibre[6] outside a living cell. If it fails, this indicates a problem with the fibre format, not the biological hypothesis. The two scientifically consistent fallbacks are (a) a living-cell hydrogel scaffold, which preserves cellular FAD replenishment, and (b) cell-surface display. Substituting CRY2 with iLOV would abandon the magnetosensory hypothesis entirely.

(1.5) Human CRY2 FAD binding affinity

Kutta et al.[4] confirmed that FAD binding and radical pair photochemistry are structurally possible in human CRY2 in vitro, which is the scientific foundation for Aim 2. The challenge is

that CRY2 binds FAD weakly (Kd 68 μM) and is predominantly unloaded in vivo,[4] and AURA's extracellular fibre has no mechanism to replenish it. The 200 μM FAD supplementation during expression maximises initial cofactor loading,[14] but retention over time is unknown. If Test 1 fails, the response protocol in order is: (a) increase FAD supplementation further; (b) engineer the FAD binding pocket by directed mutagenesis guided by Type I cryptochrome structures; (c) substitute robin CRY4, which binds FAD stoichiometrically and shows radical pair magnetosensitivity in vitro,[10] accepting loss of the human biology framing.

(2) Sweat biliverdin concentration sufficiency

Whether biliverdin in human sweat (10–100 nM) is sufficient to load DrBphP[13] is unconfirmed. The fibre's net charge of −25.85 at pH 7.4 adds an electrostatic loading barrier on top of the low sweat concentration. If biliverdin loading proves insufficient, periodic topical supplementation would be required, or DrBphP could be substituted with a chromoprotein with different cofactor requirements and visible-range output.

(3) Steric feasibility of curli assembly with large cargo

Seker et al.[6] demonstrated CsgA fusions with small cargo domains. Attaching 1,274 amino acids per monomer far exceeds that precedent, and whether CsgA can still drive self-assembly under this load; and whether the resulting fibre geometry allows CRY2 and DrBphP sufficient conformational freedom to function, remain open questions. 3D bioprinting post-extrusion is a potential alternative fabrication approach, though cell-free synthesis is not: it lacks the Type VIII secretion machinery and cellular outer membrane that CsgA requires for extracellular self-assembly.

(4) Tryptophan tetrad identity in human CRY2

The tryptophan positions forming the radical-pair electron-transfer chain in human CRY2 have not been experimentally mapped; characterised tetrad positions exist only for avian CRY4 and Drosophila CRY.[9,10] The computational candidates identified here, W311, W358, W371, W390/W393, and W416/W418, require site-directed mutagenesis for confirmation. Crucially, the Aim 2 spectroscopic assays can yield informative results without resolving this first: if all four tests pass, the mechanism is functioning regardless of which residues carry the electron.

(5) Electromagnetic framing and pseudoscience risk

Mitigation: maintain scientifically precise public language that clearly distinguishes what Foley et al.[9] and Xu et al.[10] demonstrated from what AURA hypothesises. These are distinct claims and must never be conflated.

Section 6: Additional Information

References

[1] Toyota, M. et al. (2018). Glutamate triggers long-distance, calcium-based plant defense signaling. *Science*, 361(6407), 1112–1115.

[2] Fukasawa, Y. et al. (2026). Electrical information flows across the sporocarps of two ectomycorrhizal fungi in the field. *Scientific Reports*, 16, 12397.

[3] Nelson, I. (2025). Exploring the influence of Schumann resonance and electromagnetic fields on bioelectricity and human health. *Electromagnetic Biology and Medicine*, 44(3), 348–358. doi:10.1080/15368378.2025.2508466

[4] Kutta, R.J. et al. (2017). Vertebrate cryptochromes are vestigial flavoproteins. *Scientific Reports*, 7, 44906.

[5] Engels, S. et al. (2014). Anthropogenic electromagnetic noise disrupts magnetic compass orientation in a migratory bird. *Nature*, 509, 353–356.

[6] Seker, U.O.S. et al. (2017). Synthetic Biogenesis of Bacterial Amyloid Nanomaterials. *ACS Synthetic Biology*, 6(2), 266–274.

[7] Duraj-Thatte, A.M. et al. (2021). Programmable microbial ink for 3D printing of living materials. *Nature Communications*, 12, 6600.

[8] Clarke, D. et al. (2013). Detection and Learning of Floral Electric Fields by Bumblebees. *Science*, 340(6128), 66–69.

[9] Foley, L.E., Gegear, R.J. and Reppert, S.M. (2011). Human cryptochrome exhibits light-dependent magnetosensitivity. *Nature Communications*, 2, 356. doi:10.1038/ncomms1364

[10] Xu, J. et al. (2021). Magnetic sensitivity of cryptochrome 4 from a migratory songbird. *Nature*, 594, 535–540. doi:10.1038/s41586-021-03618-9

[11] Sutton, G.P. et al. (2016). Mechanosensory hairs in bumblebees detect weak electric fields. *PNAS*, 113(26), 7261–7265.

[12] Chen, X., Zaro, J.L. and Shen, W.C. (2013). Fusion protein linkers: property, design and functionality. *Advanced Drug Delivery Reviews*, 65(10), 1357–1369.

[13] Bhoo, S.H. et al. (2001). Bacteriophytochromes are photochromic histidine kinases using a biliverdin chromophore. *Nature*, 414, 776–779.

[14] Hirano, A., Braas, D., Fu, Y.-H. and Ptáček, L.J. (2017). FAD regulates CRYPTOCHROME protein stability and circadian clock in mice. *Cell Reports*, 19(4), 255–266. doi:10.1016/j.celrep.2017.03.041

[15] Ritz, T. et al. (2004). Resonance effects indicate a radical-pair mechanism for avian magnetic compass. *Nature*, 429, 177–180.

PDB 4I6E: *Arabidopsis thaliana* CRY2 photolyase homology region crystal structure.
PDB 4GW9: *Deinococcus radiodurans* DrBphP bacteriophytochrome biliverdin-bound crystal structure.
PDB 4O0P: DrBphP Pr state crystal structure.
Addgene #69864: pET-28a expression vector.
UniProt Q49AN0: CRY2_HUMAN, *Homo sapiens*.
UniProt P28307: CsgA, Major curlin subunit, *E. coli* K12.
UniProt Q9RZA4: DrBphP, *Deinococcus radiodurans*.
AlphaFold 3 (Google DeepMind / EBI): structural prediction.
IDT Codon Optimization Tool: codon optimisation.
Claude (Anthropic): Protein Analysis, Calculations, Plan, Finding Sources, Feedback and Editing Document.

Supply List and Budget

- pET-28a expression vector (Addgene #69864) — $65
- Fragment 1: CsgA gene fragment (507 bp, Standard, Twist Biosciences) — $30.42
- Fragment 2: CRY2 gene fragment (1,515 bp, Complex, Twist Biosciences) — $90.90
- Fragment 3a: DrBphP first half (1,155 bp, Standard, Twist Biosciences) — $69.30
- Fragment 3b: DrBphP second half (1,179 bp, Complex, Twist Biosciences) — $70.74
- *E. coli* BL21(DE3) + DH5alpha competent cells (NEB) — ~$140
- HiFi DNA Assembly Master Mix NEB #E2621S — ~$90
- NdeI + XhoI restriction enzymes (NEB) — ~$60
- LB media, kanamycin, IPTG (Sigma-Aldrich) — ~$60
- Biliverdin chromophore + FAD (Sigma-Aldrich) — ~$100
- HisTrap HP His-tag purification column (Cytiva) — ~$150
- PURExpress In Vitro Protein Synthesis Kit NEB #E6800S — ~$200
- Gel extraction + miniprep kits (Qiagen/NEB) — ~$80
- Helmholtz coil 0–500 μT (Physics dept) — ~$200/day
- UV-Vis spectrophotometer (Institution) — ~$50/day
- Pulsed 455 nm LED + shutter system — ~$300–600
- Fluorescence spectrophotometer access — ~$50–100/day
- Anti-FLAG antibody + western blot reagents — ~$200–300
- Argon gas cylinder — ~$50–100
- Quartz cuvettes — ~$50–150
- Silicone mold fabrication (Aim 3, contingent) — ~$200–400
- 3D bioprinting access (Aim 3, contingent) — ~$200

Phase	Estimated Cost
Aim 1: Digital design (completed)	~$0
Aim 2: Wet lab and functional testing	~$1,707–$1,957
Aim 3: Complete garment (contingent on Aim 2)	~$300–$600
TOTAL	**~$2,007–$2,557**

Reflection

AURA began as an instinct before it became a science project. The original question, whether a living material could make electromagnetic fields perceptible to the body, felt more like a design proposition than a scientific hypothesis. The challenge of Aim 1 was translating my conceptual ideas into a tangible and applicable synthetic biology project.

The most instructive part of the process was gene synthesis. Three successive Twist Biosciences rejections forced me to understand the construct at a level that purely computational work had obscured. I had designed the EAAAK×3 linker without fully reckoning with how its three identical repeats would appear to a synthesis algorithm. I had not anticipated that CsgA's amyloid domain architecture would carry intrinsic direct repeats that cannot be diversified without breaking the protein. Resolving these problems across fourteen design phases was frustrating in the moment, but it produced a more defensible construct and a genuine understanding of why each design choice exists. If I had submitted a single, validated fragment from the start, I would not have understood the architecture as well, and I learned through each iteration.

Working across the biology of quantum sensing, bacteriophytochrome engineering, and curli fibre materials simultaneously meant I was often operating at the edges of my fluency. The FAD binding affinity question, which only became fully clear during the citation audit, is a good example: the weakness of human CRY2 as a FAD binder was present in Kutta et al. from the beginning, but its full implications for AURA's extracellular context only crystallised when I worked through the spectroscopic protocol in detail. Next time I would front-load the critical failure mode analysis before designing around it, rather than discovering the risks as constraints accumulated.

If I were starting again, I would sequence the open uncertainties and all limitations in each protein first and design backwards from them. The question of whether CsgA can self-assemble with 1,274 amino acids of cargo is the single most load-bearing unknown in the project, and its answer would determine whether Aims 2 and 3 are viable in their current form before any gene synthesis begins. Running a rapid CsgA-only cargo scaling test before committing to the full fusion protein would have been a more efficient path.

The current DrBphP output is also a significant constraint that future iterations must address. Pr (660 nm) and Pfr (740 nm) are both near-infrared, meaning Version 1 produces no visible colour change, only a signal detectable by NIR imaging equipment. This was an acceptable starting point given DrBphP's well-characterised biliverdin chemistry and its proven Pr/Pfr switching ratio, but it limits the garment to a research instrument rather than a wearable interface. Future versions would replace DrBphP with visible-range phytochrome reporters, and expand beyond a single binary switch to a multiplexed array of spectrally distinct biliverdin-binding proteins, each tuned to a different electromagnetic frequency band. The goal is a continuous chromatic vocabulary across the visible spectrum rather than a single on/off signal, a textile that does not just detect electromagnetic variation but renders it in a form that is immediately and intuitively legible to the wearer without any imaging apparatus.

The ethical framework was not an afterthought, but it could have been integrated earlier into the design decisions themselves rather than articulated after the fact. The pseudoscience risk in particular, the gap between what the literature demonstrates and what AURA proposes, deserves to be present in the design language from the first draft, not added as a mitigation at the end. The project is genuinely novel, and the claims are defensible; they are simply more powerful when the distinctions are precise from the beginning and clarify all my conceptual ideas, which sometimes are outside the scope of my knowledge.

What AURA ultimately proposes is not just a sensing device but a new category of relationship between synthetic biology and the human body. That ambition is worth defending carefully. The work of Aim 1 is a foundation, not a proof, and the most honest outcome of the computational validation is that it has made the experimental questions cleaner and more precise, and can continue to refine future questions as Aims 2 and 3 develop, further refining the directions for this project.

Ultimately, this design challenge provided invaluable insights into protein engineering and computational modelling. Moving forward, I will maintain this speculative, forward-thinking approach to continue pushing the boundaries of science and design; however, I plan to ground my ambitious concepts with more rigorous research and robust empirical findings to validate my designs.